Received: 17 April 2017 | Revised: 13 August 2017 | Accepted: 22 August 2017

DOI: 10.1002/poc.3773

RESEARCH ARTICLE

WILEY Journal of Physical Organic Chemistry

Two salts and the salt cocrystal of ciprofloxacin with thiobarbituric and barbituric acids: The structure and properties

Nicolay N. Golovnev[1] | Maxim S. Molokeev[1,2,3] | Maxim K. Lesnikov[1] | Victor V. Atuchin[4,5]

[1]Siberian Federal University, Krasnoyarsk, Russia

[2]Laboratory of Crystal Physics, Kirensky Institute of Physics, Federal Research Center KSC SB RAS, Krasnoyarsk, Russia

[3]Department of Physics, Far Eastern State Transport University, Khabarovsk, Russia

[4]Laboratory of Optical Materials and Structures, Institute of Semiconductor Physics SB RAS, Novosibirsk, Russia

[5]Laboratory of Semiconductor and Dielectric Materials, Novosibirsk State University, Novosibirsk, Russia

Correspondence
Maxim Molokeev, Laboratory of Crystal Physics, Kirensky Institute of Physics, FRC KSC SB RAS, Bld. 38 Akademgorodok 50, Krasnoyarsk 660036, Russia.
Email: msmolokeev@gmail.com

Funding information
RFBR, Grant/Award Number: 17-52-53031 and 16-52-48010

Abstract

Ciprofloxacin (CfH, $C_{17}H_{18}FN_3O_3$) crystallizes with 2-thiobarbituric (H_2tba) and barbituric acid (H_2ba) in the aqueous solution to yield salt $CfH_2(Htba)\cdot 3H_2O$ (**1**), salt cocrystal $CfH_2(Hba)(H_2ba)\cdot 3H_2O$ (**2**), and salt $CfH_2(Hba)\cdot H_2O$ (**3**). The compounds are structurally characterized by the X-ray single-crystal diffraction. The numerous intermolecular hydrogen bonds N–H···O and O–H···O formed by water molecules, $Htba^-/Hba^-$ and CfH_2^+ ions, and H_2ba molecules stabilize the crystal structures of **1** to **3**. Hydrogen bonds form a 2D plane network in the salts of **1** and **3** and a 3D network in the salt cocrystal of **2**. There are different π-π interactions in **1** to **3**. The compounds have been characterized by powder X-ray diffraction, thermogravimetry/differential scanning calorimetry, and Fourier transform infrared spectroscopy. The compounds dehydration ends at 130°C to 150°C, and their oxidative decomposition is observed in the range of 250°C to 275°C.

KEYWORDS

barbituric and thiobarbituric acids, ciprofloxacin, infrared spectroscopy, salt cocrystal, thermal stability, X-ray diffraction

1 | INTRODUCTION

Fluoroquinolones are one of the most important classes of synthetic antibiotics.[1] However, the molecular mechanism of this enzyme inhibition is still unknown.[2,3]

Ciprofloxacin (CfH), 1-cyclopropyl-6-fluoro-4-oxo-7(piperazin-1-yl)-1,4-dihydro-3-quinolinecarboxylic acid (Figure 1A), is a widely prescribed broad-spectrum oral fluoroquinolone antibiotic.[4] It forms different unstable hydrates.[5] In the aqueous solution, CfH exists predominantly as a zwitterion (isoelectric point = 7.42). Its intrinsic solubility in water at 25°C is comparatively low approximately 0.08 gL^{-1}.[6] One obvious way to increase the aqueous solubility of CfH is to make a salt.[7,8] The most common marketed form of CfH is that of the hydrochloride monohydrate. Evidently, a further search for other CfH salts with improved properties is of great practical interest in pharmacology.[9,10] Along with the salts, it is possible to use the so-called salt cocrystals[11,12] (or ionic cocrystals[13]). The term "salt cocrystal" indicates that a salt, be it inorganic and organic, can cocrystallize with an organic molecule.[14] In a cocrystal, if at least one of coformers is a drug molecule or ion, then it is termed as a pharmaceutical cocrystal.[14] Today, the discovery and exploration of pharmaceutical cocrystals and salts present a major perspective for the controlled modification of key pharmaceutical properties, such as solubility, hydroscopicity, physicochemical stability, photostability, and dissolution performance.[15]

Electronic supplementary information (ESI) available. See DOI:xxx

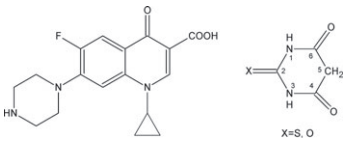

FIGURE 1 Schemes of (A) ciprofloxacin and (B) barbituric acids: X=O in H_2ba and X=S in H_2tba

Barbituric (H_2ba) and thiobarbituric (H_2tba) acids (Figure 1B) are the parent molecules of 5,5-substituted barbiturates and thiobarbiturates, respectively. H_2ba does not show any pharmaceutical activity, but its derivatives are important groups of sedative/hypnotic drugs.[16] The Hba^- and $Htba^-$ anions possess good hydrogen-bonding acceptors and donors, and this feature is important for molecular recognition and the crystal design of pharmaceuticals.[17] They can be linked by intermolecular hydrogen bonds to other complementary neutral molecules, for example, such as H_2ba and H_2tba, to form salt cocrystals.[11,18,19] Thus, salt cocrystals M(Hba)(H_2ba)·$2H_2O$ (M=Na, K), K(Hba)(H_2ba)$_{0.5}$·$1.5H_2O$,[11] and Rb(Hba)(H_2ba)·H_2O[18] were previously synthesized. The formation of cocrystals leads to an increase of the H_2ba thermal stability.[11] In the present work, for the first time, the ciprofloxacinium thiobarbiturate trihydrate, $CfH_2(Htba)\cdot 3H_2O$ (**1**), ciprofloxacinium 2-thiobarbiturate 2-thiobarbituric acid trihydrate, $CfH_2(Hba)(H_2ba)\cdot 3H_2O$ (**2**), and ciprofloxacinium barbiturate monohydrate, $CfH_2(Hba)\cdot H_2O$ (**3**), are synthesized and structurally characterized by the X-ray single-crystal diffraction. Besides, the spectroscopic and thermal properties of **1** to **3** were analyzed.

2 | EXPERIMENTAL SECTION

2.1 | Chemical reagents

Barbituric acid (CAS 67-52-7) and 2-thiobarbituric acid (CAS 504-17-6) were purchased from Sigma-Aldrich and used without further purification. Ciprofloxacinium chloride monohydrate ($CfH\cdot HCl\cdot H_2O$, Ranbaxia, India) was used without further purification.

2.2 | Synthesis

A total of 0.2 g (0.5 mmol) of ciprofloxacin hydrochloride monohydrate was dissolved in 5 mL of water, and, then, 0.074 g (0.5 mmol) H_2tba and 0.02 g (0.5 mmol) NaOH were added. The resulting mixture was heated to 80°C and held at this temperature for 30 minutes. The pale yellow bulk precipitate formed in the solution was filtered off and discarded as it consists of several phases. The hot filtrate (pH 4) was cooled to room temperature and held at 3°C for 2 days. The formed pale yellow crystal precipitate of $CfH_2(Htba)\cdot 3H_2O$ (**1**) was filtered, washed with water (1 mL) and acetone, and dried in the air (yield 30%).

The synthesis of $CfH_2(Hba)\cdot H_2O$ (**3**) was performed similar to the synthesis of **1**, except for an equimolar amount of H_2ba (0.064 g, 0.5 mmol) used instead of H_2tba. After dissolving all the reagents at 80°C, the solution was slowly cooled to room temperature (pH 4.6) and, then, the resulting colorless crystalline precipitate was filtered off, washed with water (1 mL) and acetone, and air-dried (yield 58%).

Compound $CfH_2(Hba)(H_2ba)\cdot 3H_2O$ (**2**) was obtained under similar conditions, except for that the double excess of H_2ba (0.128 g, 1.0 mmol) was used. After dissolving all the reagents at 80°C, the solution was slowly cooled to room temperature (pH 4.0) and then stored at 2°C for 24 hours. The resulting pale yellow crystalline precipitate was filtered off, washed with water (1 mL) and acetone, and air-dried (yield 60%).

The elemental analysis for $C_{21}H_{28}FN_5O_8S$ (**1**): Calc: C, 47.6%; H, 5.33%; N, 13.2%; S, 6.06. Found: C, 47.2%; H, 5.52%; N, 12.9%; S, 6.21%. The elemental analysis for $C_{25}H_{32}FN_7O_{12}$ (**2**): Calc: C, 46.8%; H, 5.03%; N, 15.3%. Found: C, 46.2%; H, 5.22%; N, 15.0%. The elemental analysis for $C_{21}H_{24}FN_5O_7$ (**3**): Calc: C, 52.8%; H, 5.07%; N, 14.7%. Found: C, 52.2%; H, 5.24%; N, 14.5%.

The single crystals suitable for structural analysis were selected directly from the total mass of precipitates **1** to **3**. The Rietveld refinement of the **1** to **3** powder patterns using crystal structures obtained from single-crystal experiments gave low *R* factors (Table S1, Figures S1 to S3). Samples **2** to **3** almost have no impurity, but sample **1** has small impurity peaks at $2\theta \sim 9.3, 14.0, 17.3, 20.8, 22.3°$. It was hard to identify impurity phase. In any case, the powder patterns of initial compounds H_2tba (I-VI forms) and CfH_2 cannot fit these peaks.

2.3 | X-ray diffraction analysis

The intensity patterns were collected from single crystals **1** to **3** using the SMART APEX II diffractometer (Bruker AXS) equipped with a charge coupled device detector, graphite monochromator, and Mo Kα radiation source. The absorption corrections were applied using the SADABS program. The structures were solved by the direct methods using package SHELXS and refined in the anisotropic approach for nonhydrogen atoms using the SHELXL program.[20] All hydrogen atoms were found via Fourier difference maps. Further, the hydrogen atoms that are linked with C,N atoms in the $Htba^-$ and CfH_2^+ ions in **1** and **2** were positioned geometrically as riding on their parent atoms with d(C–H) = 0.93 to 0.98 Å and

d(N–H) = 0.86 to 0.89 Å depending on the geometry and $U_{iso}(H) = 1.2U_{eq}(C,N)$. All hydrogen atoms of the H_2O molecules and one H atom in the OH group of CfH_2^+ ion were refined with bond length restraint d(O–H) = 0.9 Å and $U_{iso}(H) = 1.2U_{eq}(O)$. The structure test for the presence of missing symmetry elements and possible voids was produced using program PLATON.[21] The DIAMOND program is used for the crystal structure plotting.[22]

The powder X-ray diffraction data were obtained using diffractometer D8 ADVANCE (Bruker) equipped by a VANTEC detector with a Ni filter. The measurements were made using Cu Kα radiation. The structural parameters defined by single-crystal analysis were used as a base in the powder pattern Rietveld refinement.

2.4 | Physical measurements

Thermogravimetric analysis (TGA) was performed on the simultaneous SDT-Q600 thermal analyzer (TA Instruments, USA) under the dynamic air atmosphere (50-mL/min flow rate) within 25°C to 350°C at the scan rate of 10°C/min. The qualitative composition of the evolved gases was determined by Fourier transform infrared (FT-IR) spectrometer Nicolet380 (Thermo Scientific, USA) combined with a thermal analyzer and with the TGA/FT-IR interface (attachment for the gas phase analysis). This setup allows making a simultaneous accumulation of the differential thermal analysis and TG data and the composition of the released gas phase. The compound weight was 6.442 mg for **1**, 8.433 mg for **2**, and 4.442 mg for **3**. Platinum crucibles with perforated lids were used as the containers. The IR absorption spectra of the compounds inserted into the KBr tablets were recorded over the range of 400 to 4000 cm^{-1} at room temperature on an FT-IR spectrometer Nicolet 6700 (Thermo Scientific, USA, SFU CEJU).

3 | RESULTS AND DISCUSSION

3.1 | Crystal structures of 1

The unit cell of $CfH_2^+(Htba^-)\cdot 3H_2O$ corresponds to the triclinic symmetry. Space group *P*-1 was determined from the statistical analysis of the reflection intensities. The main crystal data are shown in Table 1. The corresponding bond lengths C–O, C–S, C–N, and C–C and valence angles in the CfH_2^+ cation and $Htba^-$ anion (Table S2) are well related to those found earlier for other compounds.[9,10,23–32] The asymmetrical part of the unit cell contains one CfH_2^+ ion, one $Htba^-$ ion, and 3 H_2O molecules (Figure 2A).

There are 2 intramolecular hydrogen bonds C–H···F and O–H···O and 10 intermolecular hydrogen bonds N–H···O and O–H···O in structure **1** (Figure 3A, Table 2) that form the 2D plane network. This is a 5-nodal net with stoichiometry (3-c)(3-c)(3-c)(4-c)(5-c) and with the vertex symbol $(4.5^2.6^2.7)(4.5^4.6.7^3.8)(5.6.7)(5.6.9)(5^2.7)$, which is new.[33] Hydrogen bonds form 2 alternating infinite chains. One of them consists of CfH_2^+ ions bound by water molecules; the second one consists of $Htba^-$ ions and water molecules (Figure 3A). Each CfH_2^+ ion in the chain forms H bonds with 2 water molecules, while the sequence of molecules is $CfH_2^+\cdots H_2O\cdots CfH_2^+\cdots H_2O$. When the CfH_2^+ ion interacts with one water molecule H_2(O1W), the piperazin-1-yl N atom of NH_2^+ group is the H-bond donor (N1–H···O1W), but when the CfH_2^+ ion interacts with another water molecule H_2(O2W), the O2 atom is the H-bond acceptor (H-bond O2W–H···O2). Htba ions are combined together by hydrogen bonds N–H···O into pairs with the formation of supramolecular motif $R_2^2(8)$, which is often found in other thiobarbiturate compounds.[24–31] These pairs are connected together by H bonds with the participation of 2 water molecules (cyclic motif $R_4^2(8)$), and that results in the formation of an infinite chain. Other smallest ring supramolecular motifs in this network are formed by the hydrogen bonds between ions CfH_2^+ and $Htba^-$ ($R_5^5(14)$ and $R_6^5(27)$) (Figure 3A). Also, there are π-π interactions between $Htba^-$ and CfH_2^+ rings (Table S3, Figure S4a). CfH_2^+ ions are connected in pairs by the π-π interaction of head-to-tail type.

3.2 | Crystal structure of 2

Compound $CfH_2(Hba)(H_2ba)\cdot 3H_2O$ (**2**) is a pharmaceutical cocrystal.[14] The unit cell of $CfH_2(Hba)(H_2ba)\cdot 3H_2O$ (**2**) also corresponds to the triclinic symmetry. Space group *P*-1 was determined from the statistical analysis of the reflection intensities. The main crystal data can be found in Table 1. The main bond lengths C–O, C–N, and C–C and valence angles are enumerated in Table S2. They coincide with those given in the literature for the CfH_2^+[9,10,23] and uncoordinated Hba^- ions.[34–37] The main geometric parameters of H_2ba in **2** coincided with those found in the free keto form H_2ba[38] and cocrystals.[11,18] The asymmetrical part of the unit cell contains one CfH_2^+ ion, one Hba^- ion (A), one H_2ba (B) molecule, and 3 H_2O molecules (Figure 2B). There are 2 intramolecular hydrogen bonds C–H···F and O–H···O and 12 intermolecular hydrogen bonds N–H···O and O–H···O in the structure (Figure 3B, Table 2) that form a 3D network. This is a 4-nodal net with stoichiometry (3-c)(3-c)(3-c)2(5-c) and point symbol $(4.5.6)_2(5.6^2)(5^2.6^3.8.9^4)(6.10^2)$, which is also new.[33] Intermolecular

TABLE 1 (**1**-**3**) Crystal structure parameters

Single crystal	**$CfH_2(Htba)\cdot 3H_2O$ (1)**	**$CfH_2(Hba)(H_2ba)\cdot 3H_2O$ (2)**	**$CfH_2(Hba)\cdot H_2O$ (3)**
Moiety formula	$C_{21}H_{28}FN_5O_8S$	$C_{25}H_{32}FN_7O_{12}$	$C_{21}H_{24}FN_5O_7$
Dimension (mm)	0.15 × 0.07 × 0.02	0.25 × 0.25 × 0.12	0.30 × 0.02 × 0.02
Color	Pale yellow	Pale yellow	Colorless
Molecular weight	529.54	641.57	477.45
Temperature (K)	150	150	293
Space group, *Z*	*P*-1, 2	*P*-1, 2	$P2_1/c$, 4
a (Å)	10.640 (2)	10.352 (2)	10.2756 (7)
b (Å)	10.710 (2)	10.789 (2)	18.843 (2)
c (Å)	11.476 (2)	13.440 (3)	12.049 (1)
α (°)	68.64 (3)	72.53 (3)	90
β (°)	78.31 (3)	82.41 (3)	113.364 (2)
γ (°)	84.37 (3)	78.73 (3)	90
V (Å^3)	1192.2 (5)	1399.8 (6)	2141.8 (3)
ρ_{calc} (g/cm^3)	1.475	1.522	1.481
μ (mm^{-1})	0.201	0.127	0.118
Reflections measured	13 762	15 702	10 930
Reflections independent	5464	6407	4378
Reflections with $F > 4\sigma(F)$	2920	4653	1950
$2\theta_{max}$ (°)	55.08	55.04	52.80
h, *k*, *l*—limits	$-13 \le h \le 13$; $-13 \le k \le 13$; $-9 \le l \le 14$	$-13 \le h \le 10$; $-13 \le k \le 12$; $-17 \le l \le 17$	$-10 \le h \le 12$; $-23 \le k \le 19$; $-15 \le l \le 15$
R_{int}	0.0773	0.033	0.065
The weighed refinement of F^2	$w = 1/[\sigma^2(F_o^2) + (0.0472P)^2]$	$w = 1/[\sigma^2(F_o^2) + (0.0573P)^2 + 0.2036P]$	$w = 1/[\sigma^2(F_o^2) + (0.0557P)^2]$
No. of refinement parameters	346	427	316
*R*1 [$F_o > 4\sigma(F_o)$]	0.0593	0.0433	0.0587
*wR*2	0.1052	0.1046	0.1068
Goof	0.949	1.013	0.932
ρ_{max} (e/Å^3)	0.307	0.323	0.180
ρ_{min} (e/Å^3)	−0.340	−0.273	−0.243
$(\Delta/\sigma)_{max}$	0.001	0.002	0.000

hydrogen bonds N–H···O form the chain of alternating Hba^- and H_2ba in the keto form based on the $R_2^2(8)$ pattern. In compounds $Rb(Hba)(H_2ba)\cdot 3H_2O$[18] and $M(Hba)(H_2ba)\cdot 3H_2O$ (M=Na, K),[11] the chains with sequence $H_2ba\cdots Hba^-\cdots H_2ba\cdots Hba^-$ also are formed. However, in $K(Hba)(H_2ba)_{0.5}\cdot 1.5H_2O$, sequence $H_2ba\cdots Hba^-\cdots Hba^-\cdots H_2ba$ is observed.[11] Salt cocrystals $MBr\cdot H_2ba$ (M=Rb, Cs) and $CsI\cdot H_2ba$ are characterized by the presence of H_2ba dimers linked via N–H···O hydrogen bonds.[39] Dimeric fragment $H_2tbaHtba^-$ was observed in the salt cocrystal of piperidinium ($PipeH^+$) 2-thiobarbiturate and 2-thiobarbituric acid, PipeH(Htba) H_2tba.[19] In **2**, 2 water molecules joint CfH_2^+ ions in pairs by hydrogen bonds O–H···O forming a 16-membered ring ($R_6^4(16)$). Hydrogen bonds OW–H···OW′ attract 4 water molecules (motif $R_4^4(8)$) in the cycle, 3 of which are bound by hydrogen bonds OW–HO3A with 3 Hba^- (A) ions, forming 2 bound infinite chains $\cdots Hba^-\cdots H_2ba\cdots Hba^-\cdots H_2ba$ (Figure 3B). CfH_2^+ ions are also combined into pairs by intermolecular

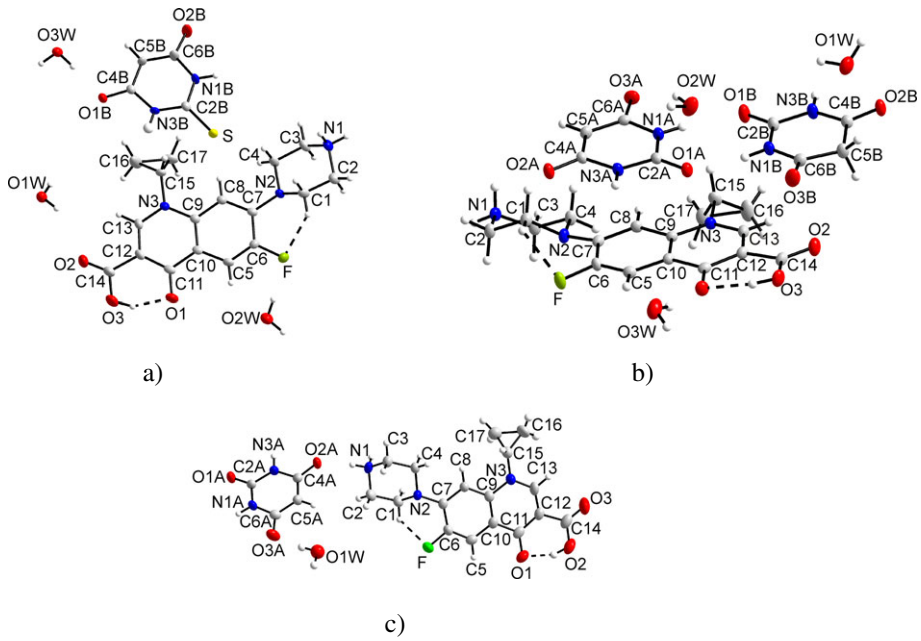

FIGURE 2 The asymmetric part of the unit cell: (A) $CfH_2(Htba)\cdot 3H_2O$ (**1**); (B) $CfH_2(Hba)(H_2ba)\cdot 3H_2O$ (**2**); and (C) $CfH_2(Hba)\cdot H_2O$ (**3**). Ellipsoids are drawn at the 50% probability level, except for the hydrogen atoms represented by spheres. The intramolecular hydrogen bonds are shown with dashed lines

hydrogen bonds OW–H···O with the participation of just 2 water molecules. Each CfH_2^+ ion is bound to Hba^- or H_2ba by a single hydrogen bond N1–H···O (Table 2). The hydrogen bonds involving Hba^- ions and H_2ba and H_2O molecules also form other cyclic motifs in this network $R_4^4(8)$, $R_5^4(14)$, and $R_6^6(20)$ (Figure 3B). There are π-π interactions between Hba^- and CfH_2^+ rings in **2**. Like in **1**, 2 CfH_2^+ form the pairs in **2** (Table S3, Figure S4b).

3.3 | Crystal structure of (3) and comparison

The unit cell of $CfH_2(Hba)\cdot H_2O$ (**3**) corresponds to the monoclinic symmetry. Space group $P2_1/c$ was determined from the systematic absences and statistical analysis of the reflection intensities. The main crystal data are summarized in Table 1. The main defined bond lengths and valence angles are shown in Table S2. They relate well to those found in **2** and in the literature for the CfH_2^+[9,10,23] and $Htba^-$ ions.[34–37] The asymmetrical part of the unit cell contains one CfH^+ ion, one Hba^- ion and one H_2O molecule (Figure 2C). There are 2 intramolecular hydrogen bonds C–H···F and O–H···O and 5 intermolecular hydrogen bonds N–H···O and O–H···O in the structure (Figure 3C, Table 2), which form a 2D network.

Hba^- ions are connected to each other by 2 hydrogen bonds N–H···O, closing the 8-membered ring ($R_2^2(8)$). As a result, they form their infinite chains along the *a* axis. With the help of H bonds N1–H···O and O–H···O, these infinite chains of Hba^- ions are joined together by other chains containing one ion CfH_2^+, H_2O, and Hba^-. The H-bond donor is the positively charged piperazinium N1 atom in CfH_2^+, which directly joints CfH_2^+ and Hba^- using H-bond N1–H···O2A. The acceptor O3 atom of CfH_2^+ carboxyl group is attracted by H-bond O1W–H11W···O3 with the water molecule, which simultaneously forms H-bond O1W–H11W···O3A with Hba^-. This is a 2-nodal net with stoichiometry $(2\text{-c})_2(4\text{-c})$ and point symbol $(6.10^5)(6)_2$, which is also new.[33] The smallest ring supramolecular motifs in this network: $R_2^2(8)$ and $R_{10}^9(52)$ (Figure 3C). Also, there are π-π interactions between the 2 rings of CfH_2^+ (Table S3, Figure S4).

It is possible to point out the similarity of the crystal structures **1** to **3**. Water molecules stabilize crystal structures **1** to **3** by forming a diverse arrangement of supramolecular heterosynthons (Figure 3). There are 2 intramolecular hydrogen bonds C–H···F and O–H···O in **1** to **3** (Figure 2). The carbonyl and carboxyl groups of CfH_2^+ are involved in a strong intramolecular O3–H···O1 hydrogen bond, and, therefore, the O3–H group does not participate in the formation of intermolecular hydrogen bonds. This limits the possibility of fluoroquinolones self-association, for example, in **1** to **3**, CfH_2^+ cations are not directly related to each other. In **2** and **3**, the CfH_2^+ ions are bound to Hba or H_2ba by hydrogen bond N1–H···O (Table 2), but in **1**, CfH_2^+ ions are bound to $Htba^-$ through bridging water molecules. Crystal structures **1** to **3** possess very similar bond lengths

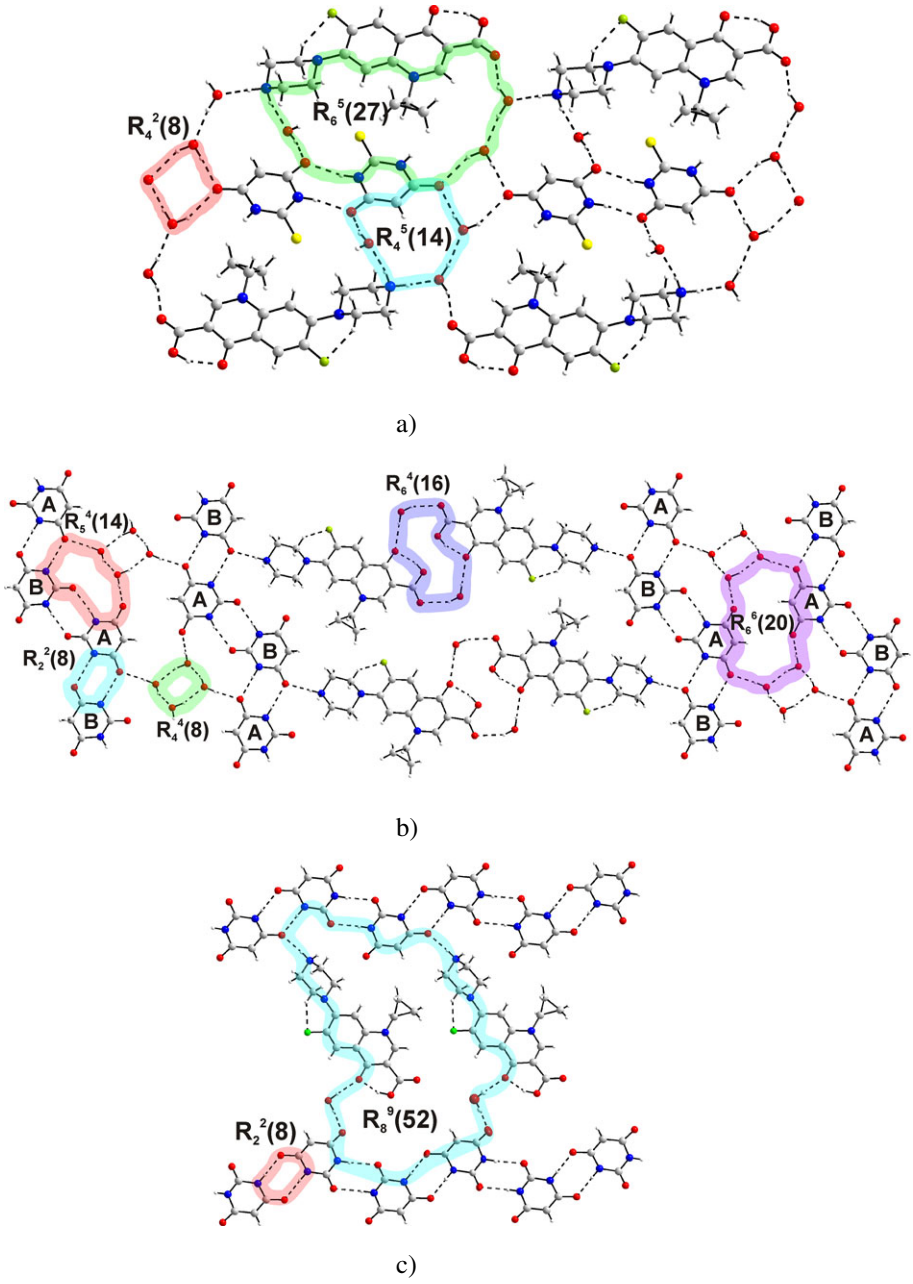

FIGURE 3 Hydrogen bonding in (A) **1**, (B) **2**, and (C) **3**. The H bonds are marked by dashed lines; the H-bond motifs are marked by circles and broad lines. Labels **A** and **B** in **2** marked Hba^- and H_2ba, respectively

O–C, C4–C5, and C5–C6 in the $O{=}C_4{-}C_5H{-}C_6{=}O$ group (Figure 2, Table S2), and that indicates the formation of the Hba^- and $Htba^-$ anions accompanied by the charge delocalization. Earlier, such delocalization was observed in other 2-thiobarbiturates[24–32] and 1,3-diethyl-2-thiobarbiturates.[40–44] Structures **1** to **3** are stabilized by π-π interactions between CfH_2^+ ions of the head-to-tail type. These interactions connect CfH_2^+ ions in pairs in structures **1** to **3** (Table S3, Figure S4). Also, there are π-π interactions between $Htba^-/Hba^-$ and CfH_2^+ ions in **1** and **2**.

3.4 | Theoretical consideration

It is generally accepted that the reaction of an acid (in our case H_2tba and H_2ba) with a base (CfH) is expected to form a salt if $\Delta pK_a = pK_a(base) - pK_a(acid) > 2$ or 3.[45] In spite of that the pK_a value describes equilibrium phenomena in the solution, it remains to be a useful parameter for preliminary prediction of the ionization state in crystals.[45]

$CfH_2^+ \rightleftharpoons CfH + H^+$ $\quad pK_a = 6.05$,[46]

$H_2tba \rightleftharpoons Htba^- + H^+$ $\quad pK_a = 1.87$,[47]

$H_2ba \rightleftharpoons Htba^- + H^+$ $\quad pK_a = 4.03$.[48]

TABLE 2 Hydrogen-bond geometry in (**1**-**3**) structures (Å, °)

D–H	d(D–H)	d(H···A)	∠ D–H···A	D···A	A	Transformation for A atom
$CfH_2(Htba)\cdot 3H_2O$ (**1**)						
O3–H3	0.90 (3)	1.70 (3)	151 (3)	2.522 (4)	O1	x, y, z
C1–H01A	0.97	2.16	128	2.861 (4)	F	x, y, z
N1–H0A	0.89	2.01	156	2.843 (3)	O2W	1 + x, y, z
N1B–H1B	0.86	1.89	168	2.734 (4)	O2B	2-x, 1-y, 1 − z
N1–H0B	0.89	1.95	169	2.827 (3)	O1W	1 − x, 1 − y, 1 − z
N3B–H3B	0.86	2.42	168	3.270 (2)	S	1 − x, 1 − y, 1 − z
O1W–H11W	0.84 (2)	2.09 (2)	169 (3)	2.918 (3)	O3W	1 − x, 2 − y, 1 − z
O1W–H12W	0.89 (3)	1.86 (3)	166 (3)	2.728 (3)	O2B	1 + x, y, z
O2W–H21W	0.91 (3)	1.91 (3)	156 (3)	2.762 (4)	O2	x, −1 + y, z
O2W–H22W	0.89 (3)	1.96 (3)	168 (3)	2.834 (3)	O3W	1 − x, 1 − y, 1 − z
O3W–H31W	0.85 (3)	2.03 (3)	156 (3)	2.829 (3)	O1B	1 − x, 2 − y, 1 − z
O3W–H32W	0.92 (3)	1.84 (3)	171 (3)	2.756 (3)	O1B	x, y, z
$CfH_2(Hba)(H_2ba)\cdot 3H_2O$ (**2**)						
O3–H3	0.87 (2)	1.70 (2)	160 (2)	2.532 (2)	O1	x, y, z
C1–H01B	0.97	2.22	125	2.894 (2)	F	x, y, z
N1–H0A	0.89	1.84	172	2.727 (2)	O3A	1 − x, 2 − y, −z
N1–H0B	0.89	1.95	168	2.832 (2)	O2B	1 + x, 1 + y, z
N1A–H1A	0.86	2.10	169	2.947 (2)	O1B	x, y, z
N1B–H1B	0.86	1.97	172	2.824 (2)	O1A	x, y, z
N3A–H3A	0.86	2.00	175	2.860 (2)	O2B	1 + x, y, z
N3B–H3B	0.86	1.91	171	2.762 (2)	O2A	1 − x, y, z
O1W–H11W	0.87 (2)	1.90 (2)	173 (2)	2.764 (2)	O2A	1 − x, 1 − y, −z
O1W–H12W	0.92 (2)	1.93 (2)	160 (2)	2.805 (2)	O2W	−x, 1 − y, −z
O2W–H21W	0.92 (2)	1.84 (2)	164 (2)	2.741 (2)	O1W	x, 1 + y, z
O2W–H22W	0.87 (2)	1.87 (2)	171 (2)	2.762 (2)	O3A	x, y, z
O3W–H31W	0.90 (2)	2.13 (2)	153 (2)	2.965 (2)	O2	1 − x, −y, 1 − z
O3W–H32W	0.94 (2)	2.08 (2)	169 (2)	3.004 (2)	O1	x, y, z
$CfH_2(Hba)\cdot H_2O$ (**3**)						
O2–H2	0.92 (3)	1.63 (4)	156 (3)	2.502 (4)	O1	x, y, z
C1–H01A	0.97	2.25	124	2.902 (4)	F	x, y, z
N1–H0A	0.89	1.83	168	2.708 (3)	O2A	x, y, z
N1A–H1A	0.86	2.09	163	2.924 (3)	O1A	1 − x, 2 − y, 1 − z
N1B–H1B	0.86	1.98	173	2.831 (3)	O2A	−x, 2 − y, 1 − z
O1W–H11W	0.94 (3)	1.84 (3)	174 (3)	2.779 (4)	O3A	x, y, z
O1W–H12W	0.92 (4)	1.94 (4)	173 (3)	2.859 (4)	O2W	−x, 1 − y, 1 − z

For reaction $H_2tba + CfH \rightleftharpoons Htba^- + CfH_2^+$,

$$K_{eq} = [Htba^-]\left[CfH_2^+\right]/[H_2tba]\,[CfH] = 10^{6.05}/10^{1.87} = 10^{4.18} \approx 1.51\cdot 10^4.$$

Therefore, the concentration of ionized species will be $1.51\cdot 10^4$ times greater than the concentration of nonionized species in an aqueous solution, containing the equimolar amounts of CfH and H_2tba. The salt formation of **1** is consistent with the ΔpK_a rule.

For reaction $H_2ba + CfH \rightleftharpoons Hba^- + CfH_2^+$,

$$K_{eq} = [Hba^-]\left[CfH_2^+\right]/[H_2ba]\,[CfH] = 10^{6.05}/10^{4.03} = 10^{2.02} \approx 105.$$

In the aqueous solution, containing the equimolar amounts of CfH and H_2ba, the ΔpK_a value for the interaction between CfH_2^+ and H_2ba is 2.02, which is also preferable for the formation of salt **3**. However, at molar ratio CfH:H_2ba = 1:2 (pH 4), the ionized and nonionized H_2ba species are coexisted in approximately equal concentrations. Thus, a favorable condition appears for the crystallization of phase **2**, containing H_2ba molecules and Hba^- anions together. The C–O distances d(O1A–C2A) = 1.235(2) Å, d(O2A–C4A) = 1.265(2) Å, and d(O3A–C6A) = 1.265(2) Å in the Hba^- ion (A) (Table S2) are greater than the C–O distances in the unionized trioxo form of H_2ba.[38] The C–O distances d(O1B–C2B) = 1.218(2) Å, d(O2B–C4B) = 1.230(2) Å, and d(O3B–C6B) = 1.206(2) Å in the H_2ba (B) molecule coincide with the distances of C–O in the molecular trioxo form of H_2ba. A similar difference between the lengths of the C–O bonds in the Hba^- ion and the H_2ba molecule was found in other salt cocrystals. For example, d(O–C) of H_2ba in salt cocrystals $Rb(Hba)(H_2ba)\cdot 3H_2O$,[18] $M(Hba)(H_2ba)\cdot 3H_2O$ (M=Na, K), $K(Hba)(H_2ba)_{0.5}\cdot 1.5H_2O$,[11] $MBr\cdot H_2ba$ (M=Na, K, Rb, Cs), and $CsI\cdot H_2ba$[39,49] are in the range of 1.21 to 1.22 Å, but these values of Hba^- are bigger, and they are in the range of 1.23 to 1.27 Å as in other compounds.[34–37,50] The distances O–C in the trioxo form of detached H_2ba (1.21-1.22 Å)[38] are similar to those in the above mentioned cocrystals and compounds $[Ca(\mu_3\text{-}H_2ba\text{–}O,O',O'')]X_2$ (X=Cl[13] and I[51]). The C–O distances d(O–C2) = 1.209 Å, d(O2–C4) = 1.269 Å, and d(HO–C6) = 1.332) Å in the H_2ba enol form show that the protonation of one of the O atoms increases the corresponding bond.[52]

The equilibrium equation for solubility **2** has the form:

$$CfH_2(Hba)(H_2ba)\cdot 3H_2O \rightleftharpoons CfH_2^+ + Hba^- + H_2ba + 3H_2O.$$

The concentration of water can be considered as almost constant, and, at pH 4, CfH exists almost completely in the form of a CfH_2^+ cation.[46] Therefore, the minimal solubility of **2** corresponds to the maximal value of the product of equilibrium concentrations $[Hba^-]\cdot[H_2ba]$ in the aqueous solution. It is easy to show that the minimal solubility should be observed under the condition of $[Hba^-] = [H_2ba]$ and at $pH = pK_a \approx 4$. Such equilibrium pH value was established immediately after the completion of crystallization **2** from the aqueous solution containing stoichiometric amounts of $CfH\cdot HCl\cdot H_2O$, H_2ba and NaOH (Section 2.2).

3.5 | IR spectroscopy

The FTIR patterns of **1** to **3** display the characteristic absorption bands of CfH and barbituric/thiobarbituric acid, showing their multicomponent crystalline composition (Figure S5). For all compounds, the resulting spectra are different from the superimposed spectra of the starting materials. These changes point out to a different set of extended hydrogen-bonding interactions for the carbonyl, hydroxyl, and amino groups present in the crystal structures. In the region of stretching vibrations υ(COOH), υ(C=O), υ(NH), and $\upsilon(NH^+)$, IR spectra contain a large number of bands that complicate their assignment.[7] Thus, the assignment of the IR vibrational bands to the corresponding normal modes is based on previous studies.[53–55] The very broad bands in the 3600 to 3400 cm^{-1} region can be assigned to the stretching modes of NH and OH groups in CfH_2^+, $Htba^-$ and Hba^- ions. The absorption bands at 1709 cm^{-1} for **1**, 1679 cm^{-1} for **2**, and 1686 cm^{-1} for **3** are attributed to the ν(COOH) vibrations in the CfH_2^+ cation.[10,55] The NH group of the piperazine ring was protonated in the crystalline compounds, and it is represented by the occurrence of medium intensity bands in the 2400 to 2700 cm^{-1} region.[10] These data suggest the salt formation by a proton transfer from the barbituric/thiobarbituric acid to CfH. In the IR spectra of H_2ba, the highest frequency band at 1752 cm^{-1} is associated with the 4,6-CO symmetric vibration ν_s(C=O).[37,54] In the IR spectra of **2**, it is observed at 1722 cm^{-1}, which agrees with the presence of the neutral H_2ba molecule, ie, with the formation of a salt cocrystal. Therefore, infrared spectroscopy gave the evidence of the salt formation in **1** and **3** and the salt cocrystal formation in **2.**

3.6 | Thermal decomposition

The thermal decomposition of **1** starts at approximately 55°C by a loss of crystal water molecules, and it is accompanied by the endo-effect at 92.6°C (Figure S6). The water removal is confirmed by the IR spectroscopic analysis of released gases. In the range from approximately 150°C to approximately 270°C, the sample mass is nearly persistent, and the mass lost (Δm) at 150°C (9.2%) almost coincides with that calculated at the assumption of 3 water molecules release (10.2%). The average value of the CfH melting temperature is equal to 270.0°C,[56,57] and H_2tba melts with the decomposition at 250.6°C.[58] Thus, compound **1** is thermally more stable than H_2tba. The melting accompanied by the oxidation of **1** occurred at $T > 270$°C, and the mass of the sample decreased rapidly in accordance to the mean TG curve. These transformations are accompanied by the endo-effect at 288.2°C and mild exo-effect above 325°C. According to the IR spectroscopic analysis of the gases evolved during thermolysis, H_2O, CO_2, NH_3, and SO_2 are formed.

In **2**, the crystal water loss starts at approximately 50°C and it is accompanied by the endo-effects at 70.2°C and 101.3°C (Figure S7). Over the range from approximately 150°C to approximately 250°C, the mass of the sample is practically unchanged, and the mass lost (Δm) at 150°C (7.6%) almost coincides with that calculated assuming the 3 water molecules release (8.4%). The sample **2** melting is accompanied by the oxidation occurred at $T > 250$°C, and the sample mass decreased rapidly at $T > 275$°C according to the mean TG curve. H_2ba melts with the decomposition at 245.0°C,[11] ie, compound **2** is more thermally stable than H_2ba. The oxidative decomposition of anhydrous organic residue is accompanied by a weak endo-effect at 288.2°C, strong exo-effect at 331.3°C, and emission of gaseous CO_2, H_2O, and NH_3.

Both TG and DSC curves of **3** indicated one-step dehydration that is accompanied by the endo-effect at 100.7°C (Figure S8). This is confirmed by the results of evolved gases IR spectroscopic analysis. The dehydration stage in the range of 70°C to 130°C showed the weight loss (Δm) equal to 2.9%, but this value is lower than the calculated weight loss estimated under the assumption of total dehydration ($-H_2O$, $\Delta m_{theor} = 3.6\%$). The underestimated Δm values for dehydration **1** to **3** are probably related to the samples partial dehydration in the air. The dehydration of **3** is accompanied by the endo-effect at 100.7°C. According to TG curves, the mass of sample **3** remains unchanged up to approximately 275°C (Figure S8) and, then, it follows by oxidative decomposition with the gaseous H_2O, CO_2, and NH_3 emissions. Similarly to **2**, compound **3** is more thermal stable than H_2ba.

Thus, the TG-DSC data confirm that compounds **1** to **3** are hydrates, and the water contents approximately correspond to the established chemical compositions.

4 | CONCLUSIONS

Ciprofloxacin crystallization with 2-thiobarbituric and barbituric acids resulted in the isolation of a new salt cocrystal (**2**) and 2 salts (**1** and **3**). The salt cocrystal is obtained in the region where the concentrations of ionized and nonionized H_2ba species are close so that both species can crystallize out. There are 2 intramolecular hydrogen bonds C–H···F and O–H···O (Figure 2) and numerous intermolecular hydrogen bonds N–H···O and O–H···O in the structures of **1** to **3** (Figure 3, Table 2). The dominant hydrogen bonding is the N–H···O interaction, which leads to a centrosymmetric synthon $R_2^2(8)$ and the formation of $Htba^-$ pairs in **1** and the infinite chains of Hba^- ions in **2** and **3**. The ciprofloxacinium cation has 6 potentially strong hydrogen bond acceptors and only 2 strong hydrogen bond donors (N atom in NH_2^+ and O atom in COOH) (Figure 1). However, the carbonyl and carboxyl groups of CfH_2^+ are involved in a strong intramolecular hydrogen bond O3–H···O1 and, consequently, the O3–H group does not form a strong intermolecular hydrogen bond. Therefore, similar to structures **1** to **3**, the self-association of fluoroquinolones with participation of O3–H group seems unlikely in other compounds. Water molecules stabilize crystal structures **1** to **3** by forming a diverse arrangement of supramolecular heterosynthons. The self-association of $Htba^-/Hba^-$ ions and the interaction of complementary Hba^- and H_2ba also stabilize the crystal structures of **1** to **3** (Figure 3). In the $O{=}C_4{-}C_5H{-}C_6{=}O$ group of Hba^- and $Htba^-$ anions, the charge delocalization is observed (Table S2). Structures **1** to **3** are stabilized by π-π interactions between CfH_2^+ ions joining them in pairs (Table S3, Figure S4).

ACKNOWLEDGEMENTS

The study was performed within the public task of the Ministry of Education and Science of the Russian Federation to the Siberian Federal University (4.7666.2017/BP) in 2017 to 2019. The reported study was funded by RFBR according to research projects 16-52-48010 and 17-52-53031. The X-ray data from single crystals were obtained with the use of the analytical equipment from the SB RAS Krasnoyarsk Center of collective use.

ORCID

Nicolay N. Golovnev http://orcid.org/0000-0002-9507-3709
Maxim S. Molokeev http://orcid.org/0000-0002-8297-0945
Maxim K. Lesnikov http://orcid.org/0000-0002-0951-5276
Victor V. Atuchin http://orcid.org/0000-0002-7424-5604

REFERENCES

[1] L. A. Mitscher, *Chem. Rev.* **2005**, *105*(2), 559.

[2] L. L. Shen, L. A. Mitscher, P. N. Sharma, T. J. Donnel, D. W. T. Chu, C. S. Cooper, T. Rosen, A. G. Pernet, *Biochemistry* **1989**, *28*, 3886.

[3] C. S. Prabodh, J. Ankit, J. Sander, *Acta Pol. Pharm-Drug Des.* **2009**, *66*, 587.

[4] J. S. Reddy, S. V. Ganesh, R. Nagalapalli, R. Dandela, K. A. Solomon, K. A. Kumar, N. R. Goud, A. J. Nangia, *Pharm. Sci.* **2011**, *100*, 3160.

[5] L. Mafra, S. M. Santos, R. Siegel, I. Alves, F. A. Almeida Paz, D. Dudenko, H. W. Spiess, *Am. Chem. Soc.* **2012**, *134*, 71.

[6] D. L. Ross, C. M. Riley, *Int. J. Pharm.* **1990**, *63*, 237.

[7] I. Turel, *Coord. Chem. Rev.* **2002**, *232*, 27.

[8] G. Zhang, L. Zhang, D. Yang, N. Zhang, L. He, G. Du, Y. Lu, *Acta Cryst. B* **2016**, *72*, 20.

[9] R. Chadha, P. Singh, S. Khullarand, S. K. Mandal, *Cryst. Growth Des.* **2016**, *16*(9), 4960.

[10] K. J. Paluch, T. McCabe, H. Müller-Bunz, O. I. Corrigan, A. M. Healyand, L. Tajber, *Mol. Pharmaceutics* **2013**, *10*(10), 3640.

[11] M. R. Chierotti, K. Gaglioti, R. Gobetto, D. Braga, F. Grepioni, L. Maini, *CrystEngComm* **2013**, *15*, 7598.

[12] S. Cherukuvada, R. Kaur, T. N. G. Row, *CrystEngComm* **2016**, https://doi.org/10.1039/c6ce1835a.

[13] D. Braga, F. Grepioni, G. I. Lampronti, L. Maini, A. Turrina, *Cryst. Growth Des.* **2011**, *11*(12), 5621.

[14] Ö. Almarsson, M. J. Zaworotko, *Chem. Commun.* **2004**, *17*, 1889.

[15] G. P. Stahly, *Cryst. Growth Des.* **2009**, *9*, 4212.

[16] E. N. Padeiskaya, *Prevention, Diagnosis, and Pharmacotherapy of Some Infectious Diseases*, Bioinform, Moscow **2002** (in Russian).

[17] K. T. Mahmudov, M. N. Kopylovich, A. M. Maharramov, M. M. Kurbanova, A. V. Gurbanov, A. J. L. Pombeiro, *Coord. Chem. Rev.* **2014**, *265*, 1.

[18] M. Gryl, K. Stadnicka, *Acta Crystallogr. E* **2011**, *67*, m571.

[19] N. N. Golovnev, M. S. Molokeev, I. V. Sterkhova, I. I. Golovneva, *J. Struct. Chem.* **2016**, *57*(6), 1266.

[20] G. M. Sheldrick, *Acta Cryst. A* **2008**, *64*, 112.

[21] *PLATON – A Multipurpose Crystallographic Tool*, Utrecht University, Utrecht, The Netherlands **2008**.

[22] K. Brandenburg, M. Berndt, DIAMOND - visual CRYSTAL structure information system CRYSTAL IMPACT, Postfach 1251, D-53002 Bonn.

[23] *Cambridge Structural Database*, Univ. of Cambridge, Cambridge, UK **2017**.

[24] N. N. Golovnev, M. S. Molokeev, *Russ. J. Inorg. Chem.* **2013**, *58*(10), 1193.

[25] N. N. Golovnev, M. S. Molokeev, I. V. Sterkhova, V. V. Atuchin, M. Y. Sidorenko, *J. Coord. Chem.* **2016**, *69*(21), 3219.

[26] N. N. Golovnev, M. S. Molokeev, M. Y. Belash, *J. Struct. Chem.* **2013**, *54*(3), 566.

[27] N. N. Golovnev, M. S. Molokeev, S. N. Vereshchagin, V. V. Atuchin, *J. Coord. Chem.* **2013**, *66*(23), 4119.

[28] N. Golovnev, M. Molokeev, *Acta Cryst. C* **2013**, *69*(7), 704.

[29] N. N. Golovnev, M. S. Molokeev, S. N. Vereshchagin, V. V. Atuchin, M. Y. Sidorenko, M. S. Dmitrushkov, *Polyhedron* **2014**, *70*, 71.

[30] N. N. Golovnev, M. S. Molokeev, *Russ. J. Inorg. Chem.* **2014**, *59*(2), 72.

[31] N. N. Golovnev, M. S. Molokeev, *Russ. J. Coord. Chem.* **2014**, *40*(9), 648.

[32] N. N. Golovnev, M. S. Molokeev, *J. Struct. Chem.* **2014**, *55*(1), 125.

[33] V. A. Blatov, A. P. Shevchenko, D. M. Proserpio, *Cryst. Growth Des.* **2014**, *14*, 3576.

[34] H. C. Garcia, R. Diniz, M. I. Yoshida, L. F. C. de Oliveira, *CrystEngComm* **2009**, *11*, 881.

[35] H. C. Garcia, R. Diniz, M. I. Yoshida, L. F. C. de Oliveira, *J. Mol. Struct.* **2010**, *978*, 79.

[36] H. C. Garcia, M. T. C. Camposa, H. G. M. Edwards, L. F. C. de Oliveira, *Vib. Spectrosc.* **2016**, *86*, 134.

[37] H. C. Garcia, F. B. de Almeida, R. Diniz, M. I. Yoshida, L. F. C. de Oliveira, *J. Coord. Chem.* **2011**, *64*, 1125.

[38] T. C. Lewis, D. A. Tocher, S. L. Price, *Cryst. Growth Des.* **2004**, *4*(5), 979.

[39] D. Braga, F. Grepioni, L. Maini, S. Prosperi, R. Gobetto, M. R. Chierotti, *Chem. Comm.* **2010**, *46*, 7715.

[40] N. N. Golovnev, M. S. Molokeev, S. N. Vereshchagin, I. V. Sterkhova, V. V. Atuchin, *Polyhedron* **2015**, *85*, 493.

[41] M. S. Molokeev, N. N. Golovnev, S. N. Vereshchagin, V. V. Atuchin, *Polyhedron* **2015**, *98*, 113.

[42] N. N. Golovnev, M. S. Molokeev, A. S. Samoilo, V. V. Atuchin, *J. Coord. Chem.* **2016**, *69*(6), 957.

[43] N. N. Golovnev, M. S. Molokeev, M. A. Lutoshkin, *Russ. J. Inorg. Chem.* **2015**, *60*(5), 572.

[44] N. N. Golovnev, M. S. Molokeev, I. I. Golovneva, *Russ. J. Coord. Chem.* **2015**, *41*(5), 300.

[45] S. L. Childs, P. Stahly, A. Park, *Mol. Pharmaceutics* **2007**, *4*(3), 323.

[46] V. M. Nurchi, G. Crisponi, J. I. Lachowicz, M. A. Zoroddu, M. Peana, S. Medici, D. Veclani, M. Tolazzi, A. Melchior, *Eur. J. Pharm. Sci.* **2016**, *93*, 381.

[47] E. Mendez, M. F. Cerda, J. S. Gancheff, J. Torres, C. Kremer, J. Castiglioni, M. Kieninger, O. N. Ventura, *J. Phys. Chem. C* **2007**, *111*(8), 3369.

[48] D. Braga, M. Cadoni, F. Grepioni, L. Maini, K. Rubini, *CrystEngComm* **2006**, *8*, 756.

[49] L. Maini, D. Braga, F. Grepioni, G. I. Lampronti, K. Gaglioti, R. Gobetto, M. R. Chierotti, *CrystEngComm* **2016**, *9*, 2950.

[50] M. Gryl, M. Koziel, K. Stadnicka, I. Matulková, I. Němec, N. Tesařová, P. Němec, *CrystEngComm* **2013**, *15*, 3275.

[51] D. Braga, F. Grepioni, L. Maini, G. I. Lampronti, D. Capucci, C. Cuocci, *CrystEngComm* **2012**, *14*, 3521.

[52] M. U. Schmidt, J. Brüning, J. Glinnemann, M. W. Hützler, P. Mörschel, S. N. Ivashevskaya, J. van de Streek, D. Braga, L. Maini, M. R. Chierotti, R. Gobetto, *Angew. Chemie Int. Ed.* **2011**, *50*, 7924.

[53] N. A. Smorygo, B. A. Ivin, *Khim. Geterotsikl. Soedin.* **1975**, *10*, 1402.

[54] J. T. Bojarski, J. L. Mokrosz, H. J. Barton, M. H. Paluchowska, *Adv. Heterocycl. Chem.* **1985**, *38*, 229.

[55] V. L. Dorofeev, *Pharm. Chem. J.* **2004**, *38*(12), 693.

[56] G. P. Vitorino, N. R. Sperandeo, M. R. Caira, M. R. Mazzieri, *Cryst. Growth Des.* **2013**, *13*, 1050.

[57] S. V. Blokhina, A. V. Sharapova, M. V. Ol'khovich, T. V. Volkova, G. L. Perlovich, *Eur. J. Pharm. Sci.* **2016**, *93*, 29.

[58] N. N. Golovnev, M. S. Molokeev, L. S. Tarasova, V. V. Atuchin, N. I. Vladimirova, *J. Mol. Struct.* **2014**, *1068*, 216.

SUPPORTING INFORMATION

Additional Supporting Information may be found online in the supporting information tab for this article.

How to cite this article: Golovnev NN, Molokeev MS, Lesnikov MK, Atuchin VV. Two salts and the salt cocrystal of ciprofloxacin with thiobarbituric and barbituric acids: The structure and properties. *J Phys Org Chem*. 2018;31:e3773. https://doi.org/10.1002/poc.3773